Int J Clin Exp Pathol 2016;9(2):611-619
www.ijcep.com /ISSN:1936-2625/IJCEP0016278

Original Article

Broad-spectrum antiviral effect of chebulagic acid and punicalagin on respiratory syncytial virus infection in a BALB/c model

Fei Xie

Department of Pediatric, Cangzhou Central Hospital, Xinhua District, Cangzhou 061000, Hebei, China

Received September 16, 2015; Accepted December 17, 2015; Epub February 1, 2016; Published February 15, 2016

Abstract: The aim of the current study was to define the Broad-spectrum antiviral effect of chebulagic acid and punicalagin on respiratory syncytial virus infection in the BALB/c model. 3-week-old female SPF BALB/c mice were infected with respiratory syncytial virus (RSV) and orally administered chebulagic acid and punicalagin. Neonatal mice showed chebulagic acid and punicalagin alleviated viral-induced lung lesions and reduced viral loads in the lung tissue in BALB/c rat with respiratory syncytial virus infection. Meanwhile, chebulagic acid and punicalagin inhibited inflammation reactions and suppressed Inducible Nitric Oxide Synthase (iNOS), cyclooxygenase-2 (COX-2) and prostaglandin E 2 (PGE2) protein expressions in BALB/c rat with respiratory syncytial virus infection. Lastly, chebulagic acid and punicalagin emerges broad-spectrum antiviral through suppression of IKK-NF-KB and MAPK signaling pathway. Our results demonstrate that the broad-spectrum antiviral effect of chebulagic acid and punicalagin on respiratory syncytial virus infection in the BALB/c model through anti-inflammation, suppression of iNOS, COX-2 and PGE2 expressions and suppression of IKK-NF-KB and MAPK signaling pathway.

Keywords: Chebulagic acid, punicalagin, respiratory syncytial virus, IKK-NF-KB, MAPK

Introduction

Respiratory syncytial virus infection is a common disease clinically. Statistics shows that more than half of acute diseases are acute upper respiratory tract infection. Adults could suffer from it 1 to 3 times each year. It is also the major cause of high morbidity and death rates worldwide [1]. Each year, about 1.9 to 2.2 million teenagers died of pneumonia all over the world [1]. Every year, each in developing countries would suffer from pneumonia for 0.29 times while the number in developed countries is 0.05 [2]. Meanwhile, it has been predicted that cases with pneumonia of teenagers less than 5 years old in China are approximately 21.1 million. Research reported that 90%-95% acute respiratory infection is caused by virus and it occupies more than 50% of emergency and outpatient cases [3]. Respiratory syncytial virus infection includes rhinitis, pharyngitis, laryngitis, amygdalitis, bronchitis, bronchiolitis and pneumonia, etc. Major causative virus constitutes of influenza virus, parainfluenza virus, respiratory syncytial virus, cytomegalovirus, adenovirus, rhinovirus, coronavirus, certain enterovirus (e.g. Coxsackie virus and ECHO virus), rubella and measles. Clinical features of respiratory viral disease are multiple [4]. Features can be slight such as common cold or upper respiratory infection (URI) while sever features can be capillary bronchitis or pneumonia or even death. It greatly threatens peoples' daily life and working [5].

Terminalia chebula Retz. belongs to combretaceae. As an important Tibetan and Mongolian medicine, it originates in provinces such as Yunnan, Guizhou, Guangdong and Guangxi [6]. It is bitter, sour and astringent in taste and neutral in nature with functions of relieving diarrhea with astringents, astringing the lung to stop cough, etc. Fruits of terminalia chebula Retz. are rich in tannins compounds accounting for about 30% to 37.36%. With strong antioxidant activities, terminalia chebula Retz. Mainly contains triterpenic acid, gallyl glucose, gallate and anthraquinone etc. New report discovered that its extracts have good antioxidant activities [7]. It was discovered that chebulagic acid and puni-

calagin could control contents of hydrogen peroxides in diabetic rats and gives play to functions of antioxygen. Chebulagic acid and punicalagin can prevent hepatic cells from oxidative damages and eliminates activities of free radicals [8]. We suggest that broad-spectrum antiviral effect of chebulagic acid and punicalagin restrains respiratory syncytial virus infection in the BALB/c model.

Materials and methods

Experimental design

This study was performed 3-week-old female SPF BALB/c mice from the Comparative Medicine Center of Yangzhou University (Yangzhou, China). BALB/c mice was housed in the Experimental Animal Center of, with a 12 h light/dark cycle, at 23 ± 2°C and freely food and water. All procedures reported in this study were reviewed and approved by the Animal Ethics Committee of Nanjing University of Chinese Medicine. 50 mice were randomly assigned into four groups: sham group (n = 12), chebulagic acid and punicalagin group (n = 12), model group (n = 12) and model + chebulagic acid and punicalagin group (n = 12). In sham group, all normal mice were gave with physiological saline from caudal vein; in chebulagic acid and punicalagin group, normal mice were gave with 50 mg/kg of chebulagic acid and 50 mg/kg of punicalagin for 24 h from caudal vein; in model group, respiratory syncytial virus infection mice were gave with physiological saline from caudal vein; in model + chebulagic acid and punicalagin group, respiratory syncytial virus infection mice were gave with 50 mg/kg of chebulagic acid and 50 mg/kg of punicalagin for 24 h from caudal vein.

Viral preparation

The A2 strain of RSV was kindly provided from Ewha Womans University, Seoul, Korea. Firstly, The RSV A2 strain propagated in HEp-2 cells and then 3-week-old female SPF BALB/c mice were intraperitoneally injected with ketamine (100 mg/kg) and xylazine (5.83 mg/kg) for anesthetization. Following anesthetization, mice were injected intranasally with 1×10^6 pfu/5 μl of RSV.

Evaluation of lung samples

Lung tissue samples were quickly acquired and wash with PBS. Tissue fluid was blotted up using filter paper. Weight of lung tissue samples were weighed "wet weight (W)" and then lung tissue samples were putted into oven at 70°C for 24-48 h and weighed as "dry weight (D)". So, content of lung tissue samples (%) = (W-D)/W × 100%.

Lung tissues histopathology

Lung tissue samples were quickly acquired and wash with PBS. Tissue fluid was fixed in 4% paraformaldehyde overnight, transferred to 70% ethanol and embedded in paraffin blocks. Lung tissue samples were quickly sectioned, in which was stained with periodic acid-Schiff (PAS).

ELISA of inflammation

The concentration of IL-1β, IL-6, IL-10 and TNF-α levels in supernatants from venous blood of very group were measured using ELISA kits in accordance with the manufacturer's instructions (BD Bioscience).

Determination of iNOS, COX-2 and PGE2 activity

Lung tissue samples were quickly acquired and wash with PBS. Tissue fluid was fixed in 4% paraformaldehyde overnight and homogenized in an ice-cold lysis buffer. After centrifugation at 12,000×g for 20 min, the supernatant was collected and conducted protein quantification by a BCA kit (Beyotime Institute of Biotechnology, Nantong, China). Equal protein was used to determined iNOS and COX-2 activity using commercial kits according to the manufacturer's instructions (Nanjing Jiancheng Biotechnology Institute, Nanjing, China) and PGE2 activity using (R&D Systems, Minneapolis, MN, USA).

Western blot analysis

Lung tissue samples were quickly acquired and wash with PBS. Tissue fluid was fixed in 4% paraformaldehyde overnight and homogenized in an ice-cold lysis buffer. After centrifugation at 12,000×g for 20 min, the supernatant was collected and conducted protein quantification by a BCA kit (Beyotime Institute of Biotechnology, Nantong, China). Equal protein was separated by electrophoresis on 8%-12% SDS-polyacrylamide gels and transferred onto nitrocellulose membranes. The membranes were blocked

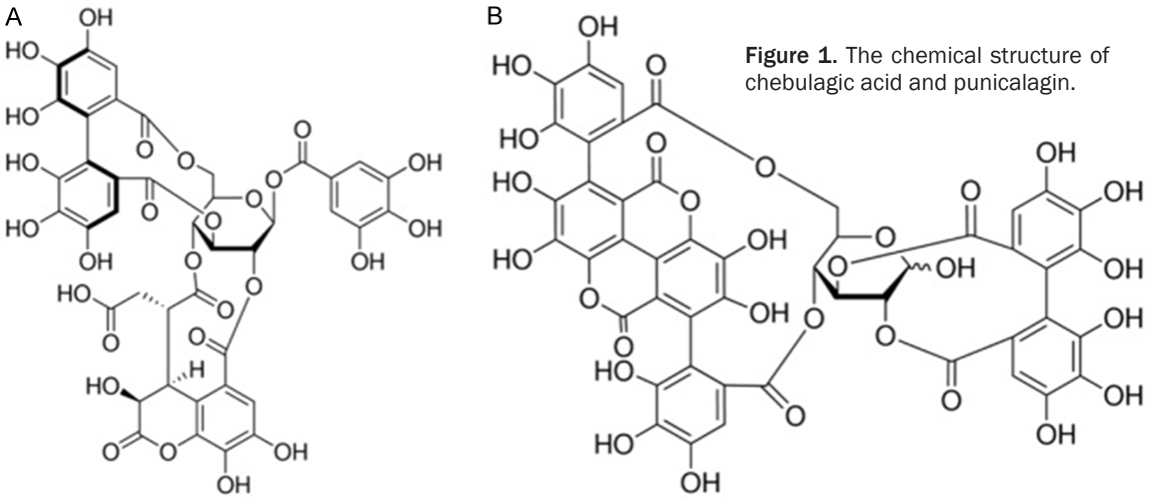

Figure 1. The chemical structure of chebulagic acid and punicalagin.

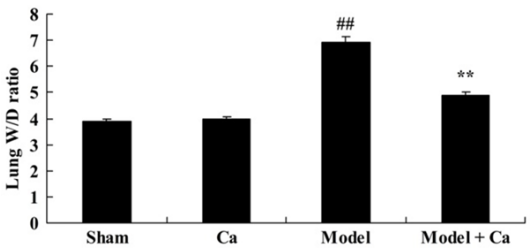

Figure 2. Broad-spectrum antiviral effect of chebulagic acid and punicalagin on lung W/D ratio in the BALB/c model. Sham, sham group; Ca, chebulagic acid and punicalagin group; Model, espiratory syncytial virus infection model group; Model + Ca, espiratory syncytial virus infection model mice + chebulagic acid and punicalagin group. ##P < 0.01 compared with sham group; **P < 0.01 compared with Model group.

with 5% skimmed milk in TBST for 1 h and Protein was detected using mouse anti-p-IKK-α (1:2000, Santa Cruz, Dallas, TX, USA) and anti-NF-KB (1:4000, Santa Cruz, Dallas, TX, USA), anti-p-38-MAPK (1:4000, Santa Cruz, Dallas, TX, USA) or mouse anti-GAPDH (1:2000, Kang Chen, Shanghai, China) overnight 4°C. Then, the membranes were blocked with horseradish peroxidase-conjugated goat antimouse antibody (1:5000, Santa Cruz, Dallas, TX, USA) and protein was conducted by Quantity One software (Bio-Rad, Hercules, CA, USA).

Statistical analysis

Data were reported as mean ± standard deviation of mean and performed with Student's t-test using the SPSS 13 (SPSS Inc., Chicago, IL, USA). The *p*-values were calculated using a two-sided, unpaired Student t-test. Values were considered to differ significantly if the *p* value was less than 0.05.

Results

Broad-spectrum antiviral effect of chebulagic acid and punicalagin on lung W/D ratio in the BALB/c model

The chemical structure of chebulagic acid and punicalagin are displayed in **Figure 1**. As shown in **Figure 2**, the lung W/D ratio of sham group was very similar to the chebulagic acid and punicalagin group. BALB/c mice were induced by respiratory syncytial virus infection exhibited a severe lung edema and higher lung W/D ratio than that of sham group (**Figure 2**). However, treatment with 100 mg/kg of chebulagic acid and punicalagin to injured mice with respiratory syncytial virus infection significantly decreased lung W/D ratio, in comparison to the respiratory syncytial virus infection model group (**Figure 2**).

Broad-spectrum antiviral effect of chebulagic acid and punicalagin on histology in the BALB/c model

On the other hand, respiratory syncytial virus infection mice showed that a severe alveolar damage than that of sham group (**Figure 3**). Meanwhile, alveolar damage of sham group was very similar to that of chebulagic acid and punicalagin group (**Figure 3**). But, treatment with chebulagic acid and punicalagin could

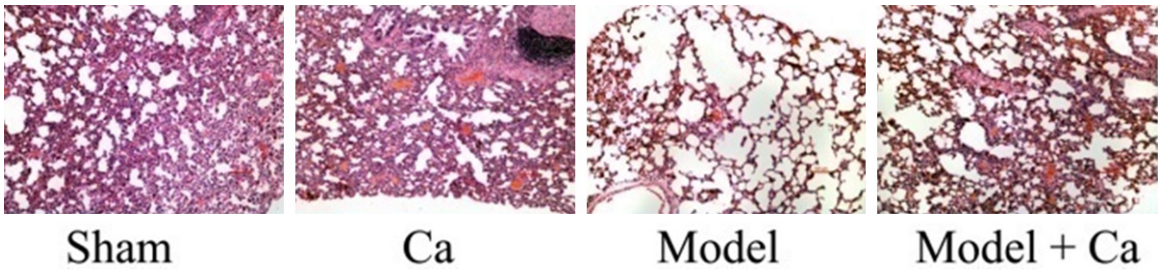

Figure 3. Broad-spectrum antiviral effect of chebulagic acid and punicalagin on histology in the BALB/c model. Sham, sham group; Ca, chebulagic acid and punicalagin group; Model, espiratory syncytial virus infection model group; Model + Ca, espiratory syncytial virus infection model mice + chebulagic acid and punicalagin group.

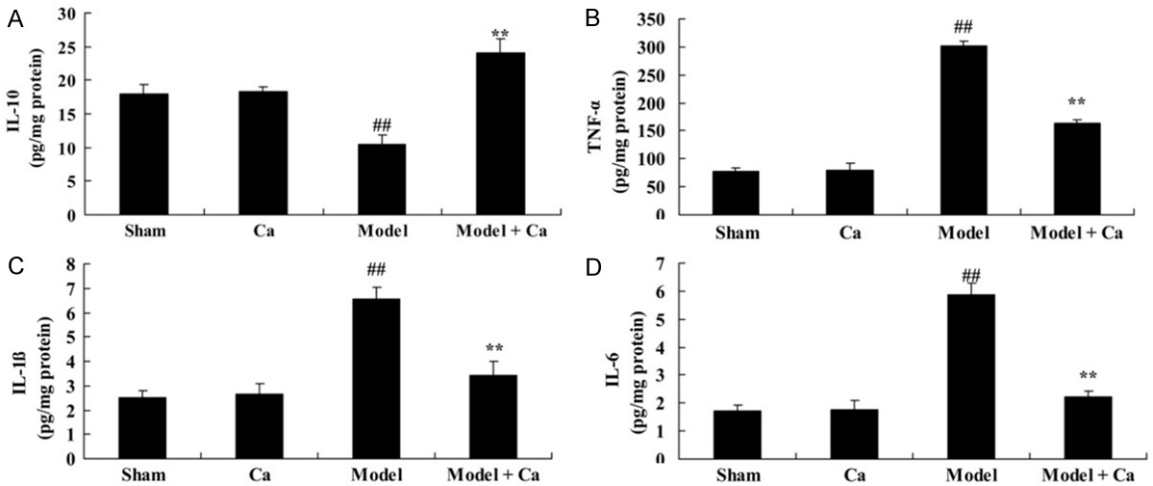

Figure 4. Broad-spectrum antiviral effect of chebulagic acid and punicalagin on inflammation in the BALB/c model. Broad-spectrum antiviral effect of chebulagic acid and punicalagin on IL-10 (A), TNF-α (B), IL-1β (C) and IL-6 (D) in the BALB/c model. Sham, sham group; Ca, chebulagic acid and punicalagin group; Model, espiratory syncytial virus infection model group; Model + Ca, espiratory syncytial virus infection model mice + chebulagic acid and punicalagin group. ##P<0.01 compared with sham group; **P < 0.01 compared with Model group.

remit the respiratory syncytial virus infection-induced alveolar damage in comparison to the respiratory syncytial virus infection model group (**Figure 3**).

Broad-spectrum antiviral effect of chebulagic acid and punicalagin on inflammation in the BALB/c model

The serum levels of IL-1β, IL-6, IL-10 and TNF-α were determined in our investigations. As shown in **Figure 4**, the serum level of IL-10 was significantly reduced and the serum levels of IL-1β, IL-6 and TNF-α were all significantly elevated in BALB/c mice induced with respiratory syncytial virus infection, compared to sham group or chebulagic acid and punicalagin group. Chebulagic acid and punicalagin treatment of respiratory syncytial virus infection-induced mice markedly suppressed these indices in comparison to the respiratory syncytial virus infection model group (**Figure 4**).

Broad-spectrum antiviral effect of chebulagic acid and punicalagin on iNOS activity in the BALB/c model

We further investigate whether chebulagic acid and punicalagin exerted protection against respiratory syncytial virus infection through mediation of iNOS activity. **Figure 5** revealed that mice-induced by respiratory syncytial virus infection showed a notable increased in the iNOS activity compared to sham group or chebulagic acid and punicalagin group. Nevertheless, chebulagic acid and punicalagin treat-

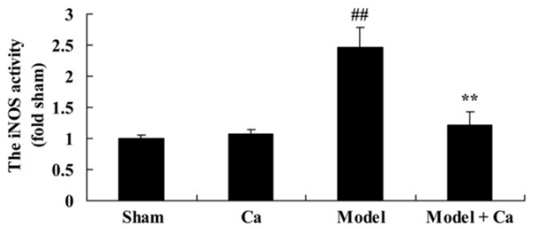

Figure 5. Broad-spectrum antiviral effect of chebulagic acid and punicalagin on iNOS activity in the BALB/c model. Sham, sham group; Ca, chebulagic acid and punicalagin group; Model, espiratory syncytial virus infection model group; Model + Ca, espiratory syncytial virus infection model mice + chebulagic acid and punicalagin group. ##P < 0.01 compared with sham group; **P < 0.01 compared with Model group.

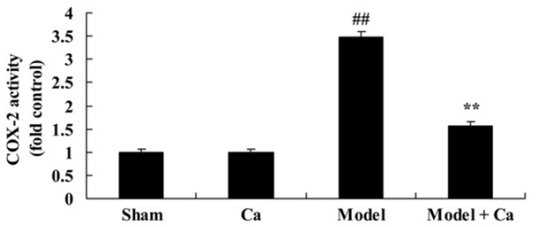

Figure 6. Broad-spectrum antiviral effect of chebulagic acid and punicalagin on COX-2 activity in the BALB/c model. Sham, sham group; Ca, chebulagic acid and punicalagin group; Model, espiratory syncytial virus infection model group; Model + Ca, espiratory syncytial virus infection model mice + chebulagic acid and punicalagin group. ##P < 0.01 compared with sham group; **P < 0.01 compared with Model group.

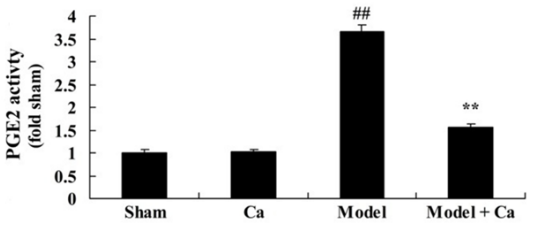

Figure 7. Broad-spectrum antiviral effect of chebulagic acid and punicalagin on PGE2 activity in the BALB/c model. Sham, sham group; Ca, chebulagic acid and punicalagin group; Model, espiratory syncytial virus infection model group; Model + Ca, espiratory syncytial virus infection model mice + chebulagic acid and punicalagin group. ##P < 0.01 compared with sham group; **P < 0.01 compared with Model group.

ment remarkably decreased the iNOS activity in respiratory syncytial virus infection mice (**Figure 5**).

Broad-spectrum antiviral effect of chebulagic acid and punicalagin on COX-2 activity in the BALB/c model

Figure 6 revealed that COX-2 activity in the BALB/c model induced respiratory syncytial virus infection were remarkably augmented compared to sham group or chebulagic acid and punicalagin group. Taken together, administration with chebulagic acid and punicalagin generated a more pronounced reduction of COX-2 activity in respiratory syncytial virus infection mice (**Figure 6**).

Broad-spectrum antiviral effect of chebulagic acid and punicalagin on PGE2 activity in the BALB/c model

Conversely, BALB/c mice induced by respiratory syncytial virus infection showed a modest increase in PGE2 activity compared to sham group or chebulagic acid and punicalagin group (**Figure 7**). Together, these data demonstrate that chebulagic acid and punicalagin treatment remarkably inhibited the respiratory syncytial virus infection-induced PGE2 activity in respiratory syncytial virus infection mice (**Figure 7**).

Broad-spectrum antiviral effect of chebulagic acid and punicalagin on IKK-NF-KB in the BALB/c model

In order to ensure the Broad-spectrum antiviral effect of chebulagic acid and punicalagin on IKK-NF-KB in the BALB/c model, Western Blot Analysis was used for further analysis. **Figure 8** revealed that respiratory syncytial virus infection increased in IKK-NF-KB in the BALB/c model compared to sham group or chebulagic acid and punicalagin group. As shown in **Figure 8**, treatment with chebulagic acid and punicalagin suppressed IKK-NF-KB signaling pathway in respiratory syncytial virus infection mice.

Broad-spectrum antiviral effect of chebulagic acid and punicalagin on p-38-MAPK in the BALB/c model

On the other hand, treatment with chebulagic acid and punicalagin showed a weak inhibition against p-38-MAPK in the BALB/c model. As shown in **Figure 9**, respiratory syncytial virus infection-induced p-38-MAPK was emerged a remarkable promotion of p-38-MAPK protein expression in the BALB/c model, compared to

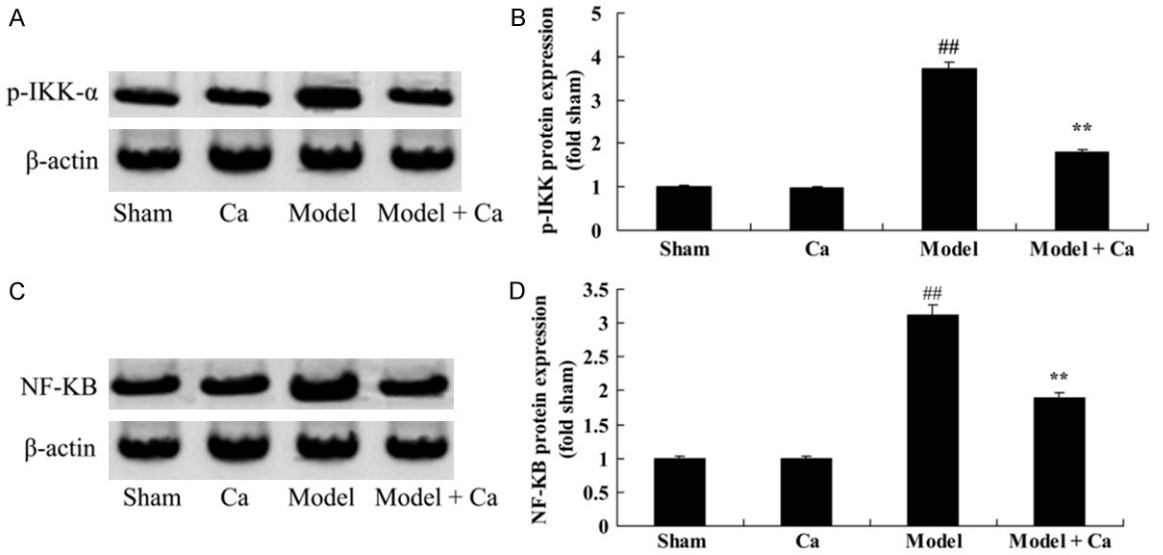

Figure 8. Broad-spectrum antiviral effect of chebulagic acid and punicalagin on IKK-NF-KB in the BALB/c model. Broad-spectrum antiviral effect of chebulagic acid and punicalagin on p-IKK-α (A) and NF-κB (C) protein expression using Western blot analysis, and statistical analysis of p-IKK-α (B) and NF-κB (D) protein expression in the BALB/c model. Sham, sham group; Ca, chebulagic acid and punicalagin group; Model, espiratory syncytial virus infection model group; Model + Ca, espiratory syncytial virus infection model mice + chebulagic acid and punicalagin group. ##P < 0.01 compared with sham group; **P < 0.01 compared with Model group.

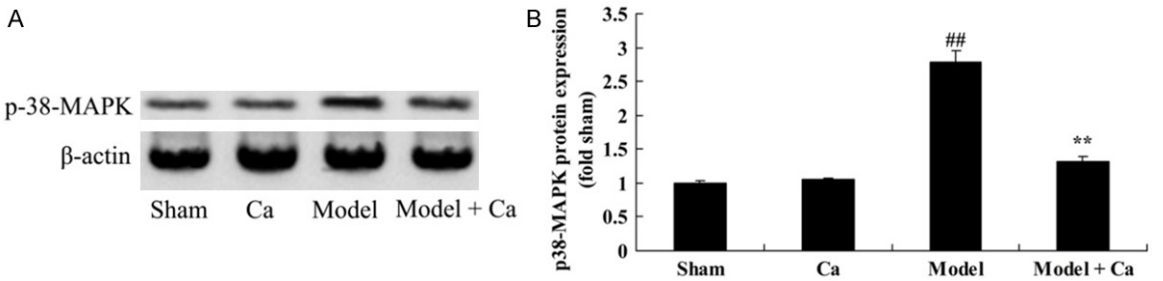

Figure 9. Broad-spectrum antiviral effect of chebulagic acid and punicalagin on p-38-MAPK in the BALB/c model. Broad-spectrum antiviral effect of chebulagic acid and punicalagin on p-38-MAPK (A) protein expression using Western blot analysis, and statistical analysis of p-38-MAPK (B) protein expression in the BALB/c model. Sham, sham group; Ca, chebulagic acid and punicalagin group; Model, espiratory syncytial virus infection model group; Model + Ca, espiratory syncytial virus infection model mice + chebulagic acid and punicalagin group. ##P < 0.01 compared with sham group; **P < 0.01 compared with Model group.

sham group or chebulagic acid and punicalagin group. However, chebulagic acid and punicalagin remarkably inhibited the p-38-MAPK protein expression of BALB/c mice with respiratory syncytial virus infection (**Figure 9**).

Discussion

Upper respiratory tract virus can invade into respiratory tracts and leads to local lesions or triggers lesions to tissues and organs by invading through respiratory tract [2]. Data shows that more than 90% of acute upper respiratory infection is caused by this kind of virus. Upper respiratory syncytial virus infection is a common and frequently-occurring disease [5]. The outbreak of SARS in 2003, bird flu and dissemination of vaccinum influenza vivum aroused great fear to people worldwide [9]. As a country with the highest rates of influenza, costs on prevention of influenza and labor loss are large. Clinical manifestations of acute upper respiratory infection are fever, rhinorrhoea, nasal obstruction, sneeze, cough, headache and pharyngalgia. Cardinal symptom is fever. Generally, it is slight with short course and good prognosis. However, its morbidity is high and is infectious. As it influences daily life and may cause

severe complications, it should be positively prevented and treated. It can be disseminated by droplet with virus or contaminated hands or apparatus. Most are sporadic and prevalent in large areas when climate has abrupt changes [10]. We previously observed the broad-spectrum antiviral effect of chebulagic acid and punicalagin weakened lung W/D ratio and alveolar damage in the BALB/c mice with respiratory syncytial virus infection. Previous research has established that chebulagic acid and punicalagin prevents against viruses in vivo [11] and viral glycoprotein-glycosaminoglycan interactions [12].

After virus infection, parasitifers can be induced to express and secrete lots of pro-inflammatory factors and immuno-regulatory molecules including the release of inflammatory mediator, necrosis of epithelial cells, occurrence of inflammation and generation of a lot of mucus [13]. Sphacelus of bronchus and bronchiole are gathered with mucus and fibrous protein, which are likely to block narrow air passages of infants [14]. Sever capillary bronchitis and pneumonia occurs or even die. In our respiratory syncytial virus infection model we showed chebulagic acid and punicalagin could reduce the respiratory syncytial virus infection-induced inflammation in mice. Reddy et al. suggested that chebulagic acid attenuates LPS-induced inflammation through p38 MAPK and NF-kappaB [8].

Under physiological status, it does not express. Simulated by endotoxin, TNF-a and IL-1, macrophage expresses iNOS, which generates lots of NO and mediates cytotoxic effects. Histocytes are injured or die [15]. Excessive NO inhibits cellular energy metabolism; improves vascular permeability; directly injuries DNA. Furthermore, it damages cell functions and structures to participate in pathological processes by activating protein kinase on cytomembrane [16]. Experiment proved that iNOS mRNA of lung tissues and metabolite of NO in douche after influenza infection are positive correlated with degrees of lung injury [17]. It suggested that excessive NO or derived products of NO takes part in lung injury. Injured cells of NO could produce lots of TNF-a and IL-1 in short period and activate mononuclear macrophage [18]. Superoxide anions are generated, which would seriously injury tissues and organs [17]. As an inflammatory medium, NO could participate in direct injury and activates NF-KB. Also, it can promote transcription of inflammatory materials and magnifies injured functions of inflammatory mediators, which would cause more serious damages to organism [19]. However, together our data conclude that the treatment with chebulagic acid and punicalagin inhibited iNOS activity in the BALB/c model of respiratory syncytial virus infection. Reddy et al. suggested that chebulagic acid attenuates LPS-induced inflammation through iNOS, COX-2, p38 MAPK and NF-kappaB [20]. Xu et al. reported that punicalagin inhibits LPS-induced inflammation through p38 and NF-κB activation [21]. Jean-Gilles et al. reported that punicalagin could reduce inflammation and type-II collagen degradation in vitro or vivo [7].

As a rate-limiting enzyme to catalyze the oxidation of arachidonic acid, COX contains COX-1 and COX-2 [22]. The production of prostaglandin induced by COX-1 participates in physiological functions and stability of internal environment in blood vessels. COX is known as inflammatory response [23]. Under normal conditions, expression of COX-2 is strictly regulated. Stimulated by growth factors, cytokines and oxidative stress, COX-2 could produce quickly in macrophages or other cells and promote the synthesis of inflammatory cells [24]. Experiment results demonstrated that after infection of macrophage by respiratory syncytial virus would up-regulate expressions of COX-2 and inflammatory medium PGE2 [25]. PGE2 causes hemangiectasis and strengthens permeability. It is closely associated with contrafluxion, edema and ache. It also can increase capacities of IL-1 and IL-2 by macrophages [25]. We have demonstrated that chebulagic acid and punicalagin suppressed the promotion of COX-2 and PGE2 activities by respiratory syncytial virus infection in the BALB/c model. Reddy et al. suggested that chebulagic acid attenuates LPS-induced inflammation through iNOS, COX-2, PGE2, p38 MAPK and NF-kappaB [20]. Achari et al. shows the chebulagic acid synergizes the cytotoxicity of doxorubicin through COX-2 and PGE2 in human hepatocellular carcinoma [26].

P38-MAPK locates at upstream of conservative cascade reactions of MAPK signal pathways. Ligand activates MAPK by this pathway and then activates MAPK [27]. After that, p38-MAPK signal pathway is activated through the phosphorization of two sites. It also participates in activating IKK-NF-KB signal pathways [28]. In this study, we found that chebulagic acid and punicalagin suppressed the respira-

tory syncytial virus infection-induced IKK-NF-KB and p38-MAPK signal pathway in mice. Achari et al. shows the chebulagic acid synergizes the cytotoxicity of doxorubicin through p38 in human hepatocellular carcinoma [26]. Kumar et al. showed that chebulagic acid ameliorates NF-κB and induces apoptosis in retinoblastoma cells [29]. Peng et al. also demonstrate that treatment with punicalagin inhibits lipopolysaccharide-induced acute respiratory distress syndrome through Toll-like receptor 4 (TLR4) expression and NF-κB activation in mice [30].

In summary, these data show the broad-spectrum antiviral effect of chebulagic acid and punicalagin ameliorates the respiratory syncytial virus infection-induced lung W/D ratio and alveolar damage in the BALB/c mice. These effects of chebulagic acid and punicalagin against respiratory syncytial virus infection revealed that anti- inflammation, and inhibition of iNOS, COX-2 and PGE2 through regulation of IKK-NF-KB and P38-MAPK signal pathway in mice.

Acknowledgements

This work was supported by Cangzhou Municipal Science and technology project (1313-02154).

Disclosure of conflict of interest

None.

Address correspondence to: Fei Xie, Department of Pediatric, Cangzhou Central Hospital, Xinhua District, Cangzhou 061000, Hebei, China. Tel: +86-15903175601; Fax: +86-15903175601; E-mail: xiefeifeifff@163.com

References

[1] Luiking YC, Poeze M and Deutz NE. Arginine infusion in patients with septic shock increases nitric oxide production without haemodynamic instability. Clin Sci (Lond) 2015; 128: 57-67.

[2] Bayar E, Ilhan G, Furat C, Atik C, Arslanoglu Y, Kuran C, Ozpak B and Durakoglugil ME. The effect of different beta-blockers on vascular graft nitric oxide levels: comparison of nebivolol versus metoprolol. Eur J Vasc Endovasc Surg 2014; 47: 204-208.

[3] Cai B, Lyu H, Huang J, Wang S, Lee CK, Gao C and Liu B. Combination of bendamustine and entinostat synergistically inhibits proliferation of multiple myeloma cells via induction of apoptosis and DNA damage response. Cancer Lett 2013; 335: 343-350.

[4] Tang SC, Lathia JD, Selvaraj PK, Jo DG, Mughal MR, Cheng A, Siler DA, Markesbery WR, Arumugam TV and Mattson MP. Toll-like receptor-4 mediates neuronal apoptosis induced by amyloid beta-peptide and the membrane lipid peroxidation product 4-hydroxynonenal. Exp Neurol 2008; 213: 114-121.

[5] Bexiga MG, Kelly C, Dawson KA and Simpson JC. RNAi-mediated inhibition of apoptosis fails to prevent cationic nanoparticle-induced cell death in cultured cells. Nanomedicine (Lond) 2014; 9: 1651-1664.

[6] Tian Y, Guo S, Guo Y and Jian L. Anesthetic Propofol Attenuates Apoptosis, Abeta Accumulation, and Inflammation Induced by Sevoflurane Through NF-kappaB Pathway in Human Neuroglioma Cells. Cell Mol Neurobiol 2015; 35: 891-898.

[7] Giovinazzo F, Turri G, Zanini S, Butturini G, Scarpa A and Bassi C. Clinical implications of biological markers in Pancreatic Ductal Adenocarcinoma. Surg Oncol 2012; 21: e171-182.

[8] Sharma HS, Ponten E, Gordh T, Eriksson P, Fredriksson A and Sharma A. Propofol promotes blood-brain barrier breakdown and heat shock protein (HSP 72 kd) activation in the developing mouse brain. CNS Neurol Disord Drug Targets 2014; 13: 1595-1603.

[9] Gaundar SS and Bendall LJ. The potential and limitations of p38MAPK as a drug target for the treatment of hematological malignancies. Curr Drug Targets 2010; 11: 823-833.

[10] Soubh AA, Abdallah DM and El-Abhar HS. Geraniol ameliorates TNBS-induced colitis: Involvement of Wnt/beta-catenin, p38MAPK, NFkappaB, and PPARgamma signaling pathways. Life Sci 2015; 136: 142-150.

[11] Pearn ML, Hu Y, Niesman IR, Patel HH, Drummond JC, Roth DM, Akassoglou K, Patel PM and Head BP. Propofol neurotoxicity is mediated by p75 neurotrophin receptor activation. Anesthesiology 2012; 116: 352-361.

[12] Lu Y, Jian M, Xiong W and Han R. [Effects of propofol on miR-181a and Bcl-2 expression in glucose deprivation cultured astrocytes]. Zhonghua Yi Xue Za Zhi 2014; 94: 3020-3023.

[13] Nouette-Gaulain K, Capdevila X and Rossignol R. Local anesthetic 'in-situ' toxicity during peripheral nerve blocks: update on mechanisms and prevention. Curr Opin Anaesthesiol 2012; 25: 589-595.

[14] Deng M, Hofacer RD, Jiang C, Joseph B, Hughes EA, Jia B, Danzer SC and Loepke AW. Brain regional vulnerability to anaesthesia-induced neuroapoptosis shifts with age at expo-

sure and extends into adulthood for some regions. Br J Anaesth 2014; 113: 443-451.
[15] Ferreira CF, Bernardi JR, da Silva DC, de Sa Couto-Pereira N, de Souza Mota C, Krolow R, Weis SN, Pettenuzzo L, Kapczinski F, Silveira PP and Dalmaz C. Mitochondrial and Oxidative Stress Aspects in Hippocampus of Rats Submitted to Dietary n-3 Polyunsaturated Fatty Acid Deficiency After Exposure to Early Stress. Neurochem Res 2015; 40: 1870-81.
[16] Tagawa T, Sakuraba S, Kimura K and Mizoguchi A. Sevoflurane in combination with propofol, not thiopental, induces a more robust neuroapoptosis than sevoflurane alone in the neonatal mouse brain. J Anesth 2014; 28: 815-820.
[17] Wang W, Lu R, Feng DY, Liang LR, Liu B and Zhang H. Inhibition of microglial activation contributes to propofol-induced protection against post-cardiac arrest brain injury in rats. J Neurochem 2015; 134: 892-903.
[18] Wu XJ, Zheng YJ, Cui YY, Zhu L, Lu Y and Chen HZ. Propofol attenuates oxidative stress-induced PC12 cell injury via p38 MAP kinase dependent pathway. Acta Pharmacol Sin 2007; 28: 1123-1128.
[19] Wang HY, Wang GL, Yu YH and Wang Y. The role of phosphoinositide-3-kinase/Akt pathway in propofol-induced postconditioning against focal cerebral ischemia-reperfusion injury in rats. Brain Res 2009; 1297: 177-184.
[20] Yeh CH, Cho W, So EC, Chu CC, Lin MC, Wang JJ and Hsing CH. Propofol inhibits lipopolysaccharide-induced lung epithelial cell injury by reducing hypoxia-inducible factor-1alpha expression. Br J Anaesth 2011; 106: 590-599.
[21] Klatka J, Grywalska E, Klatka M, Wasiak M, Andrzejczak A and Rolinski J. Expression of selected regulatory molecules on the CD83+ monocyte-derived dendritic cells generated from patients with laryngeal cancer and their clinical significance. Eur Arch Otorhinolaryngol 2013; 270: 2683-2693.
[22] Zhong Y, Liang Y, Chen J, Li L, Qin Y, Guan E, He D, Wei Y, Xie Y and Xiao Q. Propofol inhibits proliferation and induces neuroapoptosis of hippocampal neurons in vitro via downregulation of NF-kappaB p65 and Bcl-2 and upregulation of caspase-3. Cell Biochem Funct 2014; 32: 720-729.
[23] Diao HX, Jiang S, Gao PY, Liu HY, Li JN and Fan HG. Comparison of the effects of propofol and emulsified isoflurane alone or combined with dexmedetomidine on induction of anesthesia in dogs. Vet Anaesth Analg 2016; 43: 145-52.
[24] Huang Y, Chen J, Chen Y, Zhuang Y, Sun M and Behnisch T. The neurotoxin 1-methyl-4-phenylpyridinium (MPP(+)) alters hippocampal excitatory synaptic transmission by modulation of the GABAergic system. Front Cell Neurosci 2015; 9: 299.
[25] Zhao LL, Hu GC, Zhu SS, Li JF and Liu GJ. Propofol pretreatment attenuates lipopolysaccharide-induced acute lung injury in rats by activating the phosphoinositide-3-kinase/Akt pathway. Braz J Med Biol Res 2014; 47: 1062-1067.
[26] Conesa-Botella A, Meintjes G, Coussens AK, van der Plas H, Goliath R, Schutz C, Moreno-Reyes R, Mehta M, Martineau AR, Wilkinson RJ, Colebunders R and Wilkinson KA. Corticosteroid therapy, vitamin D status, and inflammatory cytokine profile in the HIV-tuberculosis immune reconstitution inflammatory syndrome. Clin Infect Dis 2012; 55: 1004-1011.
[27] Creeley C, Dikranian K, Dissen G, Martin L, Olney J and Brambrink A. Propofol-induced apoptosis of neurones and oligodendrocytes in fetal and neonatal rhesus macaque brain. Br J Anaesth 2013; 110 Suppl 1: i29-38.
[28] Yu D, Jiang Y, Gao J, Liu B and Chen P. Repeated exposure to propofol potentiates neuroapoptosis and long-term behavioral deficits in neonatal rats. Neurosci Lett 2013; 534: 41-46.
[29] Liu Y, Shi L, Liu C, Zhu G, Li H, Zhao H and Li S. Effect of combination therapy of propofol and sevoflurane on MAP2K3 level and myocardial apoptosis induced by ischemia-reperfusion in rats. Int J Clin Exp Med 2015; 8: 6427-6435.
[30] Haridas D, Chakraborty S, Ponnusamy MP, Lakshmanan I, Rachagani S, Cruz E, Kumar S, Das S, Lele SM, Anderson JM, Wittel UA, Hollingsworth MA and Batra SK. Pathobiological implications of MUC16 expression in pancreatic cancer. PLoS One 2011; 6: e26839.